Full-scale investigation of wind-induced vibrations of a mast-arm traffic signal structure

Michelle Riedman[1a], Hung Nguyen Sinh[*2], Christopher Letchford [2b] and Michael O'Rourke[2c]

[1]*Simpson Gumpertz and Heger Inc., 41 Seyon Street, Building 1, Suite 500, Waltham, MA, 02453, USA*
[2]*Department of Civil and Environmental Engineering, Rensselaer Polytechnic Institute, 110 8th St., Troy, NY, 12180, USA*

Abstract. In previous model- and full-scale studies, high-amplitude vertical vibrations of mast-arm traffic signal structures have been shown to be due to vortex shedding, a phenomenon in which alternatingly shed, low-pressure vortices induce oscillating forces onto the mast-arm causing a cross-wind response. When the frequency of vortices being shed from the mast-arm corresponds to the natural frequency of the structure, a resonant condition is created causing long-lasting, high-amplitude vibrations which may lead to the fatigue failure of these structures. Turbulence in the approach flow is known to affect the cohesiveness of vortex shedding. Results from this full-scale investigation indicate that the surrounding terrain conditions, which affect the turbulence intensity of the wind, greatly influence the likelihood of occurrence of long-lasting, high-amplitude vibrations and also impact whether reduced service life due to fatigue is likely to be of concern.

Keywords: traffic signal structures; cantilever; field monitoring; turbulence; vortex shedding

1. Introduction

1.1 Mast-arm traffic signal structures

Cantilevered mast-arm traffic signal structures, such as the one shown in Fig. 1(L), are commonly used as supports for traffic signals throughout the United States due to their practical and economical design. These structures consist of two primary structural elements: the horizontal element (referred to as the 'mast-arm') and the vertical element (referred to as the 'post'). These elements are typically made from tapered galvanized steel with hollow circular or polygonal cross sections. The mast-arm and post are connected via a 'mast-arm connection detail' in which commonly the mast-arm is welded at its end to a base plate that is bolted to a second base plate which is in turn welded to the vertical post. A typical mast-arm connection detail is shown in Fig. 1

∗Corresponding author, Ph.D. Student, E-mail: nguyeh8@rpi.edu
[a] M.S., E-mail: mariedman@sgh.com
[b] Professor, E-mail: letchc@rpi.edu
[c] Professor, E-mail: orourm@rpi.edu

(R). Mast-arm traffic signal structures are flexible with fundamental natural frequencies typically less than 1 Hz and have extremely low damping ratios, often less than 1% of critical damping.

1.2 Research problem statement

Because of their inherent flexibility and low damping, mast-arm traffic signal structures are prone to vibrations under wind loading. Once these vibrations are initiated, the structure typically undergoes a large number of cycles before the vibrations decay as a result of the low damping. Beyond simply being distracting to passing motorists, these continued vibrations cause accumulating stress cycles which can reduce the service life of the structure via fatigue.

In some cases, this fatigue can lead to a complete collapse of the mast-arm traffic signal structure. Several such collapses have occurred in recent years including over a dozen in the state of Missouri (Chen *et al.* 2003) as well as several others in Wyoming, California, and Texas (Chen *et al.* 2001). Case studies of these types of failures indicate that they occurred primarily due to fatigue at the welded connection between the mast-arm and the base plate (Chen *et al.* 2003). The fatigue cracks at the welds were observed to initiate on top of the arms which is associated with bending of the mast-arms in the vertical plane. It is also important to note that the failures of these structures did not occur during extreme-event wind conditions (Hamilton *et al.* 2000). Instead, the failures were due to fatigue crack growth due to the accumulation of damage over time caused by low speed wind-induced vibrations.

The failure of several mast-arm structures prompted the inclusion of Section 11 – Fatigue Design into the 2001 and later editions of The American Association of State Highway and Transportation Officials (AASHTO) Standard Specifications for Structural Supports for Highway Signs, Luminaires, and Traffic Signals (AASHTO 2009). In this provision, AASHTO requires design for an infinite fatigue life in which fatigue stresses must not exceed the allowable constant-amplitude fatigue threshold limits for the structural details in question.

1.3 Vortex shedding

Recent research suggests that vortex shedding is the mechanism responsible for causing large-amplitude vertical vibrations of mast-arm traffic signal structures (Letchford *et al.* 2008, Cruzado and Letchford 2013, Hua and Zuo 2012). Vortex shedding occurs when flow across a bluff body causes low-pressure vortices with alternating directions of rotation (and on opposite sides of the mast-arm) to be shed into the body's wake (Holmes 2007). This alternating change in pressure distribution creates oscillating forces on the body perpendicular to the direction of flow causing the body to vibrate in a cross-flow response as illustrated in Fig. 2. In the case of a mast-arm traffic signal structure, wind flow nominally perpendicular to the length of the mast-arm causes vibration of the mast-arm in the vertical direction. Vortex shedding occurs most coherently for uniform 2D bodies when the flow approaching is uniform with low turbulence. In contrast, gross cross-section changes or turbulence in the approach flow tends to make the shedding of vortices less regular even though the strength of the vortices is maintained (Holmes 2007).

The vortex shedding frequency (n_s, Hz) is directly proportional to the mean wind speed ($\bar{U}$) and inversely proportional to the width of the bluff-body (diameter of the mast-arm - b). The vortex shedding frequency can be expressed as a non-dimensional parameter, the Strouhal number (S_t), which is typically equal to 0.2 for circular shapes (Holmes 2007) for sub-critical Reynolds numbers. This relation is shown in Eq. (1) below.

Fig. 1 Mast-Arm Traffic Signal Structure (NYSDOT 2010) (L) and Connection Detail (R)

$$S_t = \frac{n_s b}{\bar{U}} \qquad (1)$$

If the frequency at which the vortices are shed roughly corresponds to the natural frequency of the structure, a resonant condition is reached and vibrations with high amplitudes can occur. In some cases, the vibrations of the body itself may enhance the strength of the vortices and may also alter the vortex shedding frequency tending to couple it with the natural frequency of the structure creating a phenomenon known as 'lock-in' (Holmes 2007).

1.4 Previous research

Previous studies have shown evidence that vortex shedding is the mechanism responsible for large-amplitude vibrations of mast-arm traffic signal structures. Of particular note are two studies conducted at Texas Tech University (TTU) (Letchford *et al.* 2008, Cruzado and Letchford 2013, Hua and Zuo 2012). In the first of these studies, full-scale investigations were performed utilizing two out-of-service cantilever mast-arm traffic signal structures. These were tested at Reese Technology Center Facilities of the Wind Sciences and Engineering Research Center of TTU (Letchford *et al.* 2008, Cruzado and Letchford 2013). These structures had mast-arm lengths of 18.3 m and 13.4 m. Each structure had signals with back plates mounted horizontally along the mast-arm. Wind data was recorded by a sonic anemometer mounted above each post while vibrations at the tip of each mast-arm were recorded by video cameras which tracked the motion of an infrared target.

In this TTU investigation, it was observed that large amplitude vertical vibrations of the mast-arms occurred, for the most part, at particularly low wind speed ranges (between 2.24 and 4.47 m/s), and that as the wind speed increased above this range, the amplitude of the vertical vibrations decreased. Having these large vibrations over a specific wind speed range reflects the typical behavior of vortex shedding. In this TTU study, it was also observed that higher amplitude vertical oscillations have a higher probability of occurring when the wind speed is steady (i.e., has low turbulence).

As a follow up to this TTU study, a second study, conducted at the same TTU facilities, investigated the wind-induced vibrations of mast-arm traffic signal structures with a variety of

mast-arm cross sections and signal cluster configurations (Hua and Zuo 2012). Three configurations were investigated: mast-arm with a circular cross section with signals mounted horizontally, mast-arm with a circular cross section with signals mounted vertically, and mast-arm with a 16-sided cross-section with signals mounted vertically. The full-scale data collected from this study suggested that for all three systems, the large-amplitude vibrations were induced by 'lock-in' vortex-shedding.

1.5 Research objective

In New York state, based on NYSDOT analysis, it is suggested that previously designed and installed long mast-arm traffic signal structures may not meet the fatigue provisions of the updated AASHTO code (NYSDOT, 2010). There was concern that these relatively new structures would not provide long-term reliable and safe service. For this reason, the New York State Department of Transportation (NYSDOT) commissioned Research Project No. C-10-07, "Determining Remaining Fatigue Life of In-Situ Mast-Arm Traffic Signal Supports". This project is a collaborative effort between Rensselaer and NYSDOT with the primary goal of developing a general methodology that can be used to assess the remaining fatigue life of cantilevered mast-arm traffic signal structures throughout New York state. As part of this project, a full-scale investigation was conducted to determine the response of a given, in-situ mast-arm traffic signal structure to actual, observed wind conditions. This paper focuses specifically on the aforementioned full-scale investigation component of the NYSDOT project.

2. Setup

In order to study the effects of wind induced vibrations on mast-arm traffic signal structures, a full-scale investigation was conducted on an in-situ cantilevered traffic signal structure located in Malta, New York, (approximately 40 km North of Albany, New York) in a heavily wooded suburban environment typical of upstate New York. The mast-arm of this traffic signal structure was 25 m in length, making it one of the longest in New York state. The mast-arm is tapered in diameter ranging from 432 mm at its fixed end to 288 mm at its free end. The vertical post is 5.8 m in height (5.1 m height to the mast-arm connection) and also has a tapered diameter ranging from 457 mm at the base to 421 mm at the top.

2.1 Sensors

Sensors were installed on the structure to monitor wind conditions (speed and direction) along with the corresponding vibrations of the mast-arm. The data obtained from these sensors was recorded through an on-site data acquisition system and downloaded during weekly site visits.

2.1.1 Accelerometer
A tri-axial accelerometer (Wilcoxon Research Model 993A) was installed near the tip of the mast-arm to measure the vibrations of the traffic signal structure. This accelerometer has a range of +/- 50 g, a sensitivity of 1.5 x 10-4 g, and a sampling speed of up to 2,000 Hz. The accelerometer was oriented such that the x-axis corresponded with the horizontal motion along the length of the

mast-arm, the y-axis corresponded to the horizontal motion perpendicular to the length of the mast-arm, and the z-axis corresponded to the vertical motion, as shown in Fig. 3.

2.1.2 Anemometer

To capture wind data, a 3-component ultrasonic anemometer (R.M. Young Company Model 81000) was installed near the fixed end of the mast-arm. This anemometer captures wind speeds up to 40 m/s, has a sensitivity of 0.01 m/s, and is able to record data at sampling speeds up to 32 Hz. The anemometer continuously recorded wind velocities in three directions (u, v, w) and used these to calculate wind speed, elevation angle (wind direction with respect to the horizontal plane), and azimuth angle (wind direction in horizontal plane with respect to project North). The anemometer was mounted 1.25 m above the centerline of the mast-arm in order to minimize turbulence caused by the mast-arm and surrounding electrical wires. This positioned the anemometer 6.35 m above the ground. The anemometer was oriented so that the north direction was aligned perpendicular to the orientation of the mast-arm creating a Project North which was offset from True North by 33°, as shown in Fig. 3.

2.2 Data acquisition system

The data acquisition system consisted of two primary components including a data logger and a field laptop. These devices were housed in a weatherproof lock-box which was mounted on the post of the traffic signal structure. The data logger, in combination with a field laptop, was used to collect and store data from these sensors as individual 15-minute long time history files.

2.2.1 Data logger

A data logger (Delphin Technology Top Message Data Logger with ADVT module) was used to continuously collect 6 channels of data (marked with corresponding date and time stamps) from the sensors at a rate of 23 Hz, a factory preset. This data logger has an A/D convertor with a 14 bit resolution. The six data channels included accelerations in the x, y, and z directions from the accelerometer along with wind speed, elevation angle, and azimuth angle from the anemometer.
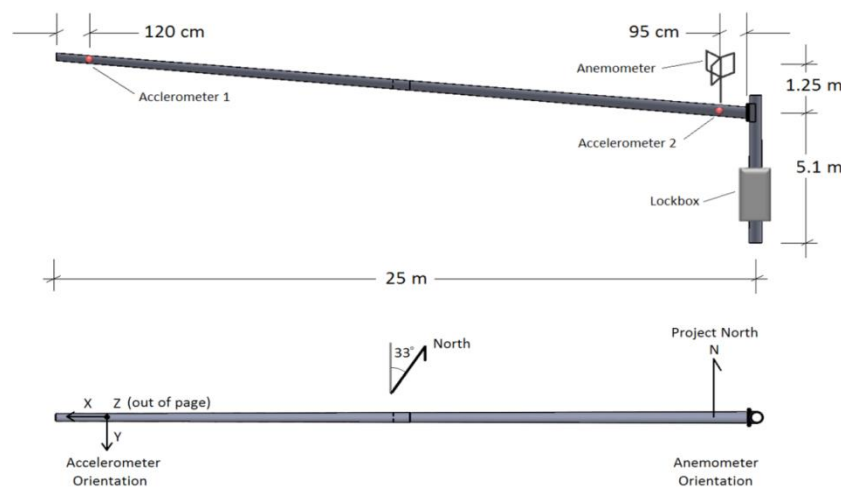

Fig. 3 Instrumentation Layout and Sensor Orientations - Elevation View (Top), Plan View (Bottom)

2.2.2 Field computer

A field laptop (Dell semi-rugged Latitude E6430 ATG) was programmed to save 15-minute increments of the continuously recorded data from the data logger into individual date and time stamped files. A 'rugged' laptop was chosen for its ability to safely operate within an extreme range of temperatures (0 to 32°C) an important consideration for the upstate New York climate. An indoor/outdoor thermometer was used to record the high and low temperatures reached both inside and outside of the lock-box between each site visit to ensure safe operating conditions were maintained for the field computer.

3. Dynamic characteristics

Prior to choosing the instrumentation plan for the full-scale investigation, a finite element computer model of the traffic signal structure was created using the ABAQUS/CAE© in order to estimate the natural frequencies and corresponding mode shapes of vibration. The natural frequency results from the finite element model were compared with the measured natural frequencies obtained through free vibration tests.

3.1 Finite element model creation details

3.1.1 Geometry

The finite element model of the structure consisted of six individual parts with tied boundary conditions (no slip and no rotation) applied to the surfaces connecting adjacent parts. The six parts included two parts for the mast-arm (one for each side of the existing slip joint connection), the vertical post, and three parts for the connection detail between the mast-arm and the vertical post. Details such as the taper of the mast-arm, the taper of the vertical post, the mast-arm connection details, and the mast-arm slip joint detail were also included in the model.

Dimensions of the traffic signal structure for use in the finite element model were taken from construction plans provided by NYSDOT. Measurements of the structure were also taken during the installation of the sensors and indicated that the structure was constructed in accordance with the contract drawings.

3.1.2 Material properties

Typical material properties for ASTM A572 Gr 65 steel, as specified on the plans provided, were used and applied as solid homogeneous sections throughout the model. These material properties included a mass density equal to 7850 kg/m^3, Young's Modulus equal to 200 GPa, and Poisson's Ratio equal to 0.25.

3.1.3 Mesh properties

General purpose three-dimensional linear hexahedral elements were used for the model's mesh. Specifically, type C3D8R elements were used, each consisting of 8 nodes, 6 faces, and a single integration point located in the center of the element. A moderate number of nodes (3156) and elements (1649) were used in the model to provide a balance between accuracy and computational cost. The elements used for the mast-arm were sized such that the arm was sectioned into 50 segments along its length (each with a length equal to 0.5 meters) and 8 segments around its circumference. The mast-arm connection detail was meshed with a higher nodal density to ensure

an accurate calculation of stresses and strains in this highly stressed region.

3.1.4 Traffic signals

Vertically hung traffic signals were assumed to act as point masses and were therefore added to the finite element model as concentrated nodal masses. The locations of the traffic signals along the length of the mast-arm were obtained from a combination of photographs and field measurements. The masses of the traffic signals were estimated to be 27 kg for single sets of signals and 54 kg for multi-sets (T. P. Products 2013) and were applied along the centerline of the mast-arm.

3.1.5 Foundation

The NYSDOT plans indicated that the traffic signal structure is attached to the foundation by four bolts which provide flexibility in each of the three Cartesian directions by a combination of their tensile, flexural, and shear behavior. This flexibility was modeled through the application of four springs to the base of the FEM structure. These springs had directionally independent stiffness values which were specified for the lateral and longitudinal directions. These stiffnesses were determined from equilibrium, compatibility, and constitutive relations applicable to the tensile behavior of the bolts (for stiffness in the blots' longitudinal direction) and flexural and shear behavior of the bolts (for stiffness in the bolts' transverse direction). The resulting stiffness equations are shown in Eqs. (2) and (3) where E is the elastic modulus, G is the shear modulus, A is the cross sectional area of a bolt, and L_e is the effective length of a bolt. The resulting bolt springs were 2.5 x 10^7 N/m in the lateral (horizontal) directions and 4.9 x 10^8 N/m in the longitudinal (vertical) direction at each bolt.

$$k_{long} = \frac{EA}{L_e} \qquad (2)$$

$$k_{lat} = \frac{1}{\frac{L_e^3}{12EI} + \frac{L_e}{AG}} \qquad (3)$$

3.2 FEM results

Modal analyses were performed on the finite element model in order to determine the natural frequencies and mode shapes of the structure. Through these analyses, it was determined that the model had a fundamental natural frequency of 0.51 Hz for vibration in both the vertical direction and the horizontal direction. Second mode natural frequencies were calculated as 2.1 Hz (Vertical Direction) and 2.3 Hz (Horizontal Direction) which are unlikely to be excited by the wind since the first mode shape is more consistent with the expected deflected shape of the mast arm subject to vortex shedding. The fundamental mode shapes for vibrations in the vertical and horizontal directions are shown in Fig. 4. If the bolt stiffnesses were ignored, the natural frequencies estimated for this condition (fully fixed) were 0.55 Hz (vertical) and 0.66 Hz (horizontal).

3.3 Free vibration tests

3.3.1 Method

Directly following the installation of the sensors and the data acquisition system, free vibration tests were performed in order to validate the natural frequencies and to determine the damping

ratios of the traffic signal structure in both the horizontal (y) and vertical (z) directions. To conduct these tests, the tip of the mast-arm was accessed via a boom lift and the structure was manually excited into a resonant response and released into free vibration. During the free vibration phase, the accelerations at the tip of the mast-arm were recorded through the data acquisition system. The free vibration tests were repeated twice for each direction (y, z).

3.3.2 Natural frequencies

The data collected from the free vibration tests was used to plot Fourier amplitude spectra in order to determine the fundamental natural frequency of the structure in the horizontal and vertical directions. In the case of free vibration, the lowest peak seen on a Fourier amplitude spectrum indicates the natural frequency of the system. The test results indicated a natural frequency of 0.49 Hz in the horizontal (y) direction and 0.52 Hz in the vertical (z) direction. The acceleration time history response and corresponding Fourier amplitude spectrum for a free vibration test in the z-direction are shown in Fig. 5.

3.3.3 Damping ratios

The damping ratios of the structure for vibration in each direction were calculated using the acceleration time history data from the free vibration tests and the logarithmic decrement method shown in Eq. (4).
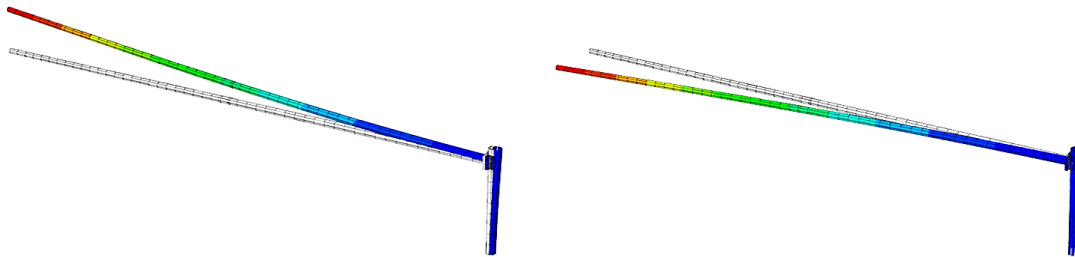

Fig.4 Fundamental Modes of Vibration: Vertical (L) and Horizontal (R)
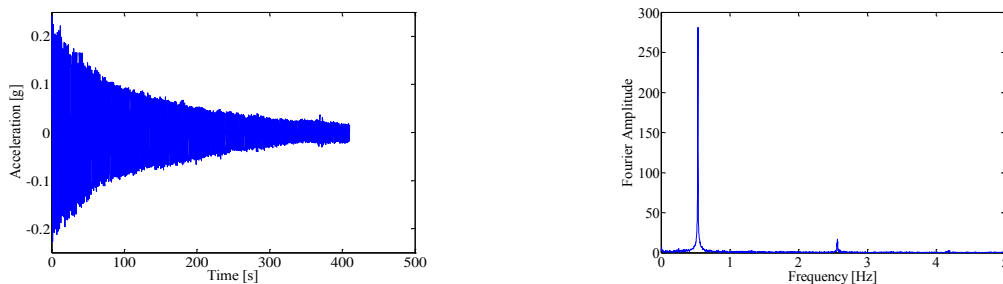

Fig. 5 Free Vibration Test: Acceleration Time History (L) and Fourier Amplitude Spectrum (R)

$$\xi = \frac{ln\left(\frac{\ddot{u}_i}{\ddot{u}_{i+j}}\right)}{2j\pi} \qquad (4)$$

In this equation, $\ddot{u}_i$ and $\ddot{u}_{i+j}$ are the accelerations at two given peaks in the acceleration time history and j is the number of cycles between the two peaks. To avoid experimental error, numerous peaks were used for the damping ratio calculations. The damping ratio of any given structure is typically dependent on the structure's amplitude of vibration. This is because at different vibration amplitudes, different mechanisms for dissipating energy are engaged. For this structure, high amplitude vibrations were defined as those having a magnitude above 0.10 g for the z-direction and 0.05 g for the y-direction. Table 1 summarizes the damping ratios obtained from the free vibration tests.

Fig. 6(L) shows the decay envelope obtained from the calculated damping ratios for the vertical direction overlaid on the corresponding acceleration time history response. In addition, Fig. 6(R) shows simultaneous vibrations in the y- and z-directions during a free vibration test in the z-direction. The small amplitude of the vibrations in the y-direction can mostly be attributed to noise from the accelerometer indicating that there was no energy transfer to other vibration modes during the test and that the decay of the vibrations in the z-direction was solely due to damping. Determining accurate damping ratios is often difficult in practice, but the important conclusion was that this structure, as expected, has very little damping. During the free vibrations tests, the structure oscillated for upwards of 10 minutes before the vibrations dissipated.
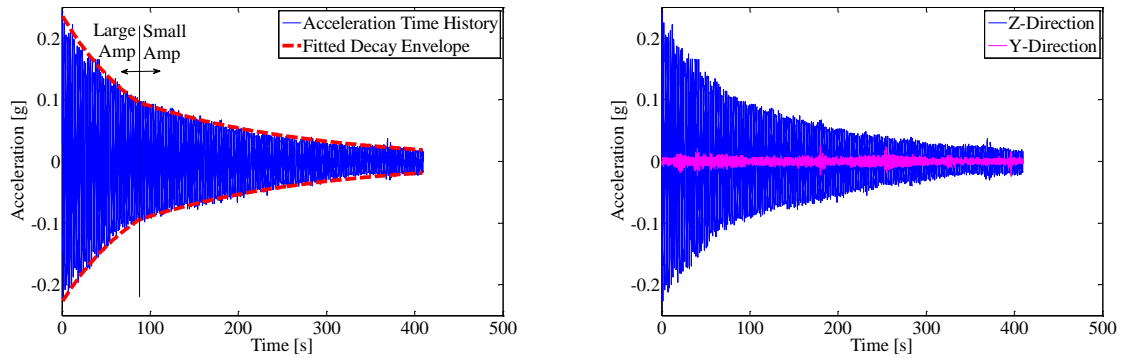

Fig. 6 Free Vibration Test: Overlaid Decay Envelope (L) and Y and Z Accelerations (R)

Table 1 Damping ratios

Test	High Amplitude	Low Amplitude	Test	High Amplitude	Low Amplitude
Z1	0.22%	0.18%	Y1	0.51%	0.54%
Z2	0.33%	0.16%	Y2	0.72%	0.42%
Z Avg	0.28%	0.17%	Y Avg	0.62%	0.48%

Table 2 Natural frequency comparison

	Vertical (Z-direction)	Horizontal (Y-direction)
Free Vibration Tests	0.52 Hz	0.49 Hz
FEM: Semi-Rigid BC	0.51 Hz	0.51 Hz
Percent Error	3.8 %	2.0 %
FEM: Fully Fixed BC	0.55 Hz	0.66 Hz
Percent Error	7.8 %	32.0 %

3.4 Comparison of results

Table 2 provides a comparison of the natural frequencies calculated from the finite element model to those determined from the free vibration tests. As shown in this table, there is reasonable agreement between the two fundamental frequency values for each direction with errors less than 5%. It should be noted, however, that if an assumption of fully fixed boundary conditions is made, rather than considering base flexibility due to the anchor bolts, the natural frequencies in both directions are overestimated by the FEM with significant error (32.0%) for the y-direction.

3.5 Estimated critical wind speed

When vortex shedding is the mechanism responsible for large amplitude vibrations of the mast-arm in the vertical direction, the largest vibrations occur due to a resonant condition when the vortex shedding frequency is equal to the natural frequency of the structure. Results from the free vibration tests were used along with the vortex shedding expression (Eq. (1)) to estimate a critical wind speed at which resonance was most likely to occur. The Strouhal number (St) was taken to be 0.2, a typical value for circular shapes (Holmes 2007). Since the mast-arm of the structure of interest is tapered, an average diameter of 0.360 m was used for the width of the bluff-body (b). The resulting estimated critical wind speed corresponding to resonance for this particular diameter was 0.9 m/s.

4. Observed wind conditions

After the collection of over 14 months of data from the full-scale investigation (from June 5, 2012 to August 22, 2013), the observed wind conditions were plotted in the form of a wind rose which shows the probability (displayed on the radial axis) that the wind blows from a particular direction (as indicated by the circumferential axis) exceeding a particular speed (as indicated by the color band and legend).

4.1 Observed project wind rose

To create the observed project wind rose, average wind speeds and wind directions were calculated for 120-second increments of data. The wind directions were defined with respect to 'Project North' based on the orientation of the anemometer which was offset from 'True North' by an angle of 33° (see Section 2). A cumulative frequency matrix was created using corresponding

average wind speeds and directions. In this matrix, each cell indicated the frequency of occurrence of a particular wind speed being exceeded from a certain direction range (10°) within the data set. The values in this matrix were plotted radially to create the observed project wind rose shown in Fig. 7(L). Fig. 7(R) shows the wind rose overlaid on the project site map. As shown in this figure, the prevailing wind direction (WNW) aligns with the more open terrain seen at the site (open grass for approximately 150 m) and possible funneling along the road to the West (Rt 67).

4.2 Comparison to long-term mean wind climate at Albany, NY Airport

Historical '2-minute mean hourly' wind speed data from August 1, 1995 to December 31, 2010 was collected from the NCDC (National Climatic Data Center) Integrated Surface Database (ISD, NCDC) for the Albany International Airport NWS (National Weather Service) station, the closest first order NWS station to the investigation site. In the case of the NCDC database, 'mean hourly' wind speeds refer to 2-minute mean wind speed recorded at the top of each hour. August 1, 1995 was selected as the start date for this historical analysis since it corresponded to the introduction of ASOS (Automated Surface Observing System) for the Albany station, a system which standardized observing practices, codes, and reporting standards for surface weather observations (NOAA 1998). The data for the Albany NWS station was recorded at a height of 10 m in flat open terrain. A wind rose was created using the NCDC 2-minute mean hourly wind speed data for the Albany NWS station and is shown in Fig. 8.

The historical wind rose at the Albany station (Fig. 8) was modified to compare with the observed wind rose at Malta. The historical 2-minute mean wind speeds at Albany Airport were modified for change in terrain and height to the Malta site. This was done by multiplying the wind speeds by a reduction factor being the ratio between the wind speed for Exposure Category B ASCE 7-10 (ASCE 2010) at the height of 6.35m (corresponding to terrain conditions in Malta and the height of the project anemometer) and the wind speed for Exposure Category C at the height of 10m (corresponding to the historical wind data at Albany). The reduction factor was expressed in Eq. (5) and was applied uniformly for all wind directions. The modified historical wind rose is shown in Fig. 9 along with the observed wind rose from the full-scale investigation data.

$$RF = \frac{Speed\ at\ Malta}{Speed\ at\ Airport} = \frac{0.45}{0.65} \times \left(\frac{6.35}{10}\right)^{1/4} = 0.618 \tag{5}$$
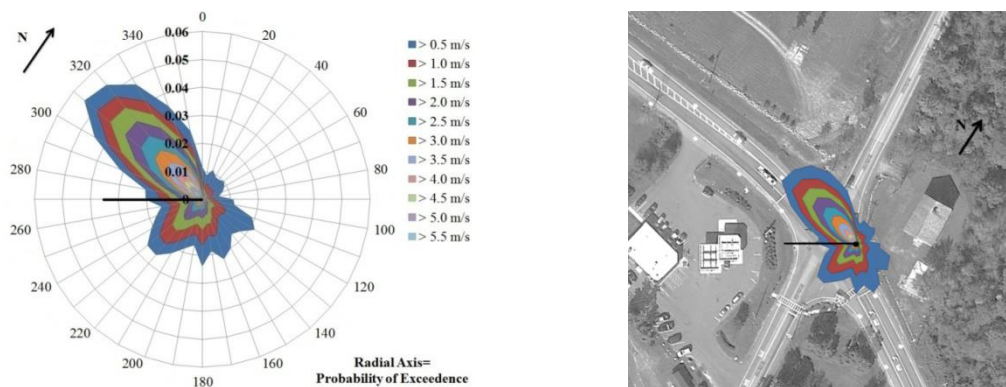

Fig. 7 Observed project wind rose at Malta, NY (left); Wind rose outline on project site map (right)
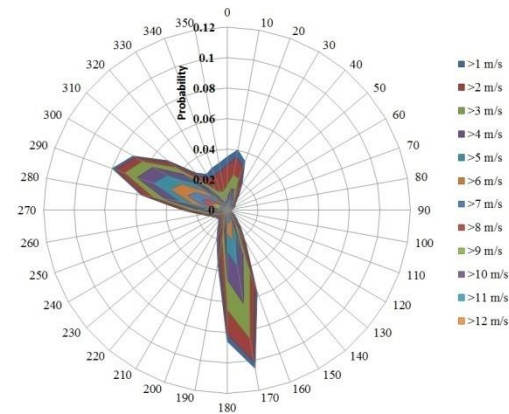
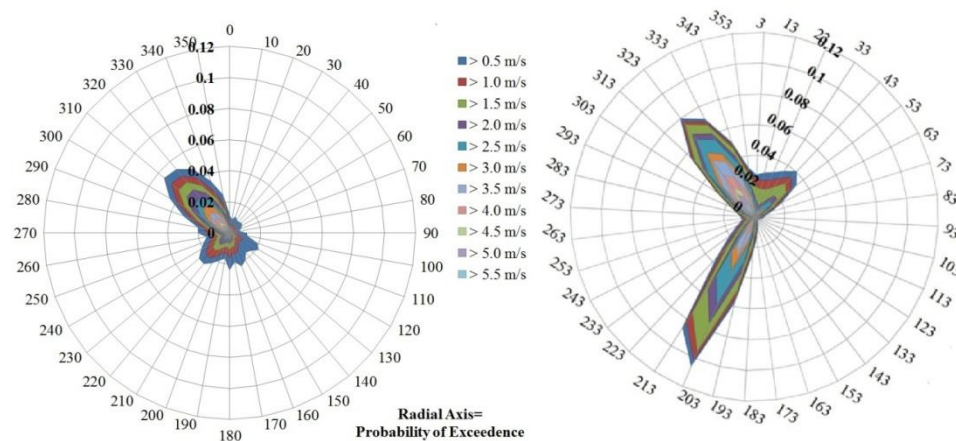Fig. 8 Historical wind rose for Albany (NY) International Airport

Fig. 9 Observed project wind rose at Malta (left), and estimated wind rose at Malta (right)

The historical wind rose at Albany was rotated clockwise by 33 degrees to align it with Project North. When the terrain and height correction factors are applied, there are still some significant differences between these two wind roses e.g., the disappearance of two other prevailing wind directions (40° and 200° from Project North) due to more significant upwind sheltering than anticipated by the terrain corrections recommended by ASCE7. This is likely because a single reduction factor has been applied uniformly across all wind directions which is clearly not correct for the Malta site and does account for specific local sheltering which would need a wind tunnel test to resolve. Another reason for the difference may be the much shorter duration of data for this investigation (one year) compared to 15 years at Albany Airport (ISD, NCDC). Those problems need to be considered while trying to use the historical wind data instead of actual wind data at the sites.

5. Results

5.1 Methodology

As noted above, wind and vibration data was collected through the full-scale investigation during a 14 month period spanning between June 2012 and August 2013. For analysis, the raw data, originally collected into 15-minute time history files, was further divided into 60-second time periods for which incremental summary statistics were calculated. These summary statistics included root-mean-square (RMS) accelerations for each of the three principle directions (x, y, and z), average wind speed (arithmetic mean), average wind elevation (arithmetic mean, typically approximately equal to zero), and average wind direction (circular average).

Fig. 10 shows an example of a raw 15-minute time history file which contains the vertical response (acceleration) of the mast arm, the horizontal response, the wind speed in the direction perpendicular to the mast arm (these wind speeds were calculate base on the wind direction and azimuth angle). Between the 20 and 170 second marks in this time history file, critical wind speed (0.9 m/s) were reached, however the vertical response was limited and the vortex shedding was not observed. This may be due to the turbulence of the wind speed or the low vortex shedding forces associated with the low critical wind speed. Both these issues are examined in more detail later in this paper.
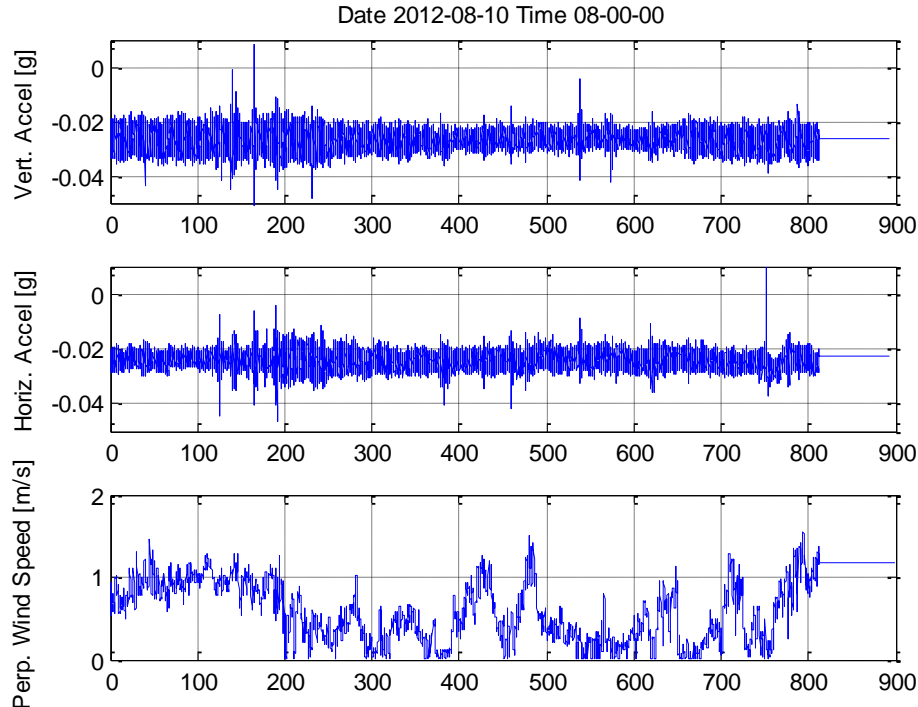

Fig. 10 Typical raw time history of data collected

After the raw data was collected from the field, several quality measures were taken to ensure uncontaminated data was used for analysis. These measures included performing baseline corrections and removing erroneous readings in the records. Specifically baseline corrections were used when the data records (i.e., acceleration records) show oscillations about a non-zero axis (as shown in Fig. 10 for vertical and horizontal acceleration) which is likely due to the accelerometer not being perfectly level in the field. Also, due to the nature of the electronics within accelerometers, occasionally large erroneous acceleration spikes are seen in the time history files. To ensure that uncontaminated data is being used for analysis, these spikes were removed from the data set by isolating the 30 second increment during which these spikes occurred and removing the corresponding data (e.g., remove spikes at around 140 and 160 second mark in Fig. 10). Finally, steps were taken to remove any time segments during which the system 'froze' while recording data (e.g., remove the last 90-seconds of the time history in Fig. 10).

5.2 Vibration vs. Wind speed results

Fig. 11 shows RMS accelerations (for 60 second time increments) corresponding to vertical vibrations (z-direction, cross-wind response) and horizontal vibrations (y-direction, along-wind response) of the mast-arm plotted against 60 second average wind speeds.

5.3 Perpendicular wind component

To account for the fact that the response of the mast arm is a combined function of wind speed and wind direction rather than just the scalar wind speed, resolved wind speeds were computed consisting of the horizontal component of the wind acting perpendicular to the mast-arm. These values were calculated using the scalar wind speed (V) and the azimuth angle (θ).

Fig. 12 shows the RMS vertical and horizontal accelerations plotted against 60-second mean perpendicular wind speeds. By using this resolved component of the wind, rather than the scalar wind speed, the values on the RMS Acceleration vs. Wind speed plots tended to shift to the left with the most severe shifts being when the average wind direction is nominally parallel to the mast arm (i.e., the same acceleration corresponding to a lower speed).
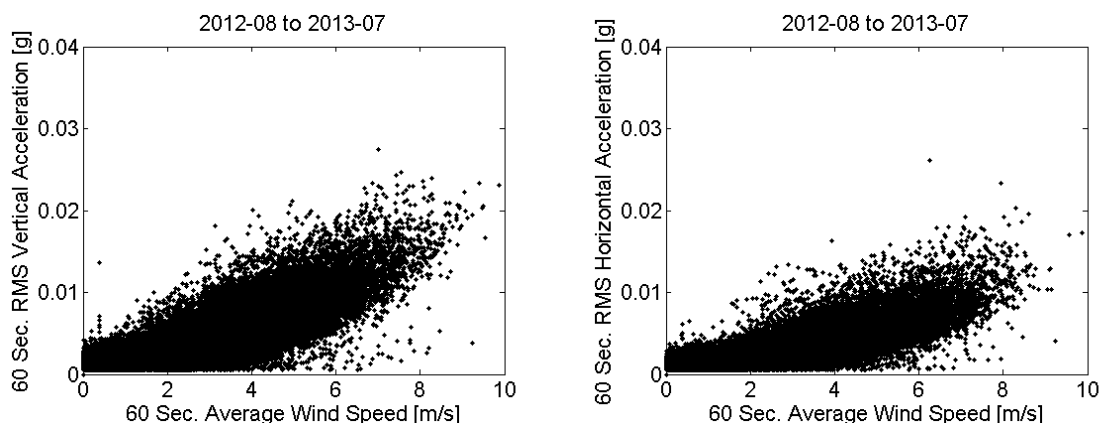

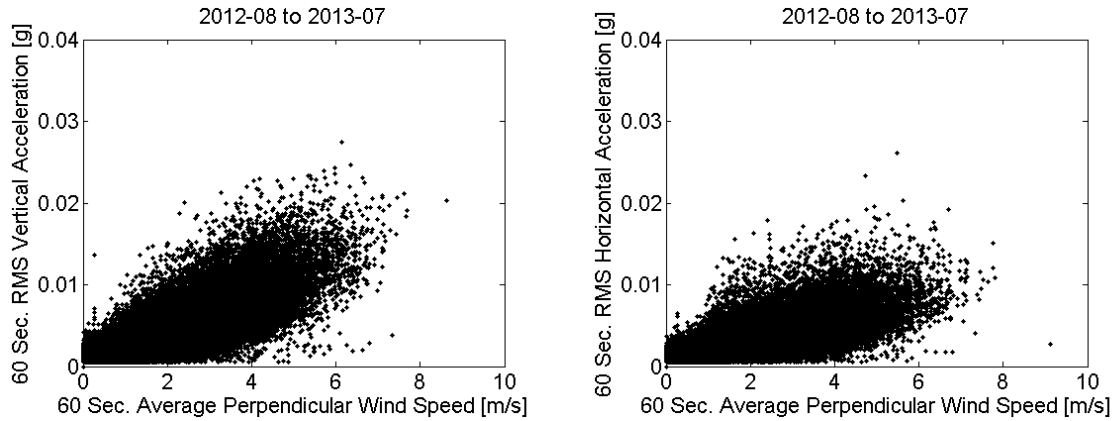Fig. 11 Vertical response (left) and horizontal response (right) versus scalar wind speed

Fig. 12 Vertical response (left) and horizontal response (right) versus perpendicular wind speed component

6. Discussion

6.1 Wind climate & Terrain

The results from this full-scale investigation show a general relationship of increasing structural response with increasing wind speed (Figs. 11 and 12). However, no clear sign of vortex shedding was observed in this investigation as shown by the lack of strong response at the critical velocity of approximately 0.9 m/s. A possible reason for the differences seen between this investigation and the tests conducted at TTU (Letchford *et al.* 2008, Cruzado and Letchford 2013, Hua and Zuo 2012) is due to the differences in terrain which surround the two field sites. At the investigation site in Malta, the surrounding conditions are classified by ASCE 7-10 (ASCE 2010) as predominately Exposure Category B which is described as "urban and suburban areas, wooded areas, or other terrain with numerous closely spaced obstructions having the size of single-family dwellings or larger". At the TTU investigation site, the surrounding terrain are classified as ASCE 7-10 Exposure Category C which is described as "open terrain with scattered obstructions having heights generally less than 9.1 m including flat open country and grasslands" (ASCE 2010). The TTU site may even be closer to Exposure D "flat, unobstructed areas and water surfaces".

Another possible reason for the difference in response may be the fact that the critical wind speed at Malta was so low (~ 0.9 m/s) that the alternating forces were also very low, resulting in vortex shedding induced mast arm vibration at Malta not being observed. In contrast, the critical wind speed for the TTU (Letchford *et al.* 2008, Cruzado and Letchford 2013, Hua and Zuo 2012) was much higher (5 m/s), one expects that the alternating forces would also be much higher, leading to easily observed vortex induced mast arm displacements.

6.2 Turbulence intensity

The amount of surface roughness, which is characterized by the ASCE Exposure Category,

influences the turbulence intensity of the wind. Turbulence Intensity is defined as the ratio of the standard deviation of the fluctuating wind speed in the mean wind direction to its mean value as expressed in Eq. (6) (Holmes 2007)

$$I_u = \frac{\sigma_u}{\bar{U}} \qquad (6)$$

The ASCE 7-10 load standard (ASCE 2010) includes a relationship presented in Eq. (7) between the turbulence intensity at a height z (in meters) and the surrounding terrain. In Eq. (7), c is an exposure category parameter equal to 0.2 for Exposure C and 0.3 for Exposure B.

$$I_{\bar{z}} = c \left(\frac{10}{\bar{z}}\right)^{\frac{1}{6}} \qquad (7)$$

The probability of occurrence of various turbulence intensities observed in the full-scale investigation conducted in Malta is shown in Fig. 13. The majority of the turbulence intensities for this project ranged from 0.1 to 0.4 (10 to 40%) with the average turbulence intensity equal to 0.32. This average turbulence intensity matches the expected turbulence intensity from ASCE 7-10 for Exposure Category B at a height of 6.4 meters as calculated by Eq. (7).

In contrast to the high turbulence intensity values observed at Malta, much lower turbulence intensities were seen in the investigations conducted at TTU. The majority of the turbulence intensities fell below 10% (Hua and Zuo 2012). In addition, results from TTU showed that the high amplitude vibrations occurred during low turbulence wind conditions with the highest of these vibrations occurring at turbulence intensities around 7% (Hua and Zuo 2012). These low turbulent conditions were rarely observed in the Malta study as indicated in Fig. 13.

Because turbulence in the approach flow tends to make the shedding of vortices less coherent since any particular critical wind speed is less sustained, the higher turbulence wind observed in this full-scale investigation are likely the reason why high-amplitude vertical vibrations, which typically reflect a vortex shedding behaviour, were not observed. The low damping ratio, roughly a quarter to a half of a percent of critical, also plays a role. Low damping results in a long ring down time as shown in Figs. 5 and 6, but also means a long ramp-up time between wind speed initially at the critical velocity and the attainment of full resonant response. Such long time frames are rare in highly turbulent flow.
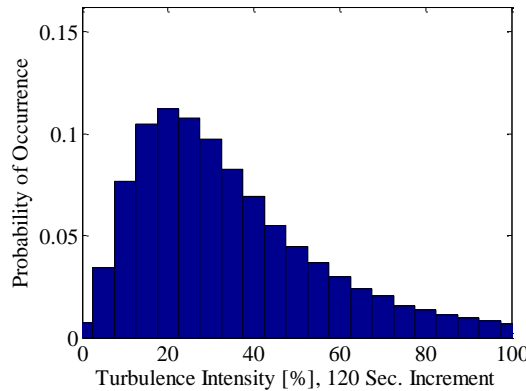

Fig. 11 Observed turbulence intensity distribution at Malta, NY

7. Conclusions

As part of a larger study aimed at determining the remaining fatigue life of in-situ mast-arm traffic signal structures, a full-scale investigation was conducted to investigate the response of a given in-situ mast-arm traffic signal structure (located in Malta, New York) to actual, observed wind conditions.

An anemometer was installed on the structure to measure wind speed and wind direction while an accelerometer was mounted at the tip of the mast-arm to record the corresponding vertical and horizontal vibrations. A finite element model was developed to predict the dynamic characteristics of the structure which were confirmed through free vibration tests. The natural frequency of the structure was used to predict the wind speed at which a resonant condition was likely to occur, through the vortex shedding mechanism.

Wind and vibration data from the full-scale investigation was collected over a 12 month period during which a general relationship of increasing response with increasing wind speed was observed. Sustained critical wind velocities leading to very large sustained vibrations due to structural resonance were not observed. When comparing the results obtained by this full-scale investigation to the results obtained from similar investigations at Texas Tech University (TTU), which do show sustained vortex shedding behavior studies (Letchford *et al.* 2008, Cruzado and Letchford 2013, Hua and Zuo 2012), it was observed that there were significant differences in the turbulence intensities observed at the two project sites. These turbulence intensity differences were caused by distinctly different surrounding site conditions as categorized by ASCE 7-10 Exposure Categories. High turbulence is known to impact the organization or coherency of vortex shedding. In addition, in highly turbulent flow, the wind does not remain steadily at the critical velocity for extended periods of time. This particularly affects lightly damped structures, such as mast-arm traffic signal structures, where there is a long ramp-up period before full resonant behavior occurs (Chopra 2007). Without a full resonant response, the structure is unlikely to experience prolonged high-amplitude vibrations and is less likely to have a reduced service life due to structural fatigue.

The other significant difference between the Malta full-scale investigation and similar investigations at TTU is the critical wind speed for vortex shedding. The critical wind speed for the Malta site (~0.9 m/s) was about an order of magnitude lower than that for the TTU site (~5 m/s). It is expected that the alternating vortex shedding force on the mast-arm is an increasing function of the critical wind speed. Based upon this alone, one would expect larger vortex shedding mast-arm vibration at TTU than at the Malta site.

Although more investigation needs to be conducted before it can be concluded that mast-arm traffic signal structures in areas of rougher suburban type terrain are not prone to large vertical vibrations due to vortex shedding and are not subject to a reduced service life, it can certainly be concluded that, for the structure in question located in Malta during the time period of study, large vibrations were a non-issue.

Acknowledgements

References

AASHTO (2009), Standard Specifications for Structural Supports to Highway Signs, Luminaires, and Traffic Signals. American Association of State Highway and Transportation Officials.

ASCE (2010), Minimum Design Loads for Buildings and Other Structures. Reston, VA: Amer. Soc. of Civil Eng.

Chen, G., Barker, M., Dharani, L.R. and Ramsay, C. (2003), *Signal mast arm fatigue failure investigation*, Missouri Dept. of Transportation, Tech. Rep..

Chen, G., Wu, J., Yu, J., Dharani, L.R. and Baker, M. (2001), "Fatigue assessment of traffic signal mast arms based on field test data under natural wind gusts", Transportation Research Rec.: *J. of the Transportation Research Board*, **1770**, 188-194.

Chopra, A K. (2007), Dynamics of Structures. Upper Saddle River, NJ: Pearson Prentice Hall.

Cruzado, H.J. and Letchford, C.W. (2013), "Full-scale experiments of cantilever traffic signal structures", *Wind Struct.*, **17**(1), 21-41.

Hamilton, H.R., Riggs III, G.S. and Puckett, J.A. (2000), "Increased damping in cantilevered traffic signal structures", *J. Struct. Eng*., **126**(4), 530-537.

Holmes, J.D. (2007), *Wind Loading of Structures*, 2nd Ed., London, Taylor and Francis.

Hua, J. and Zuo, D. (2012), "Wind-induced vibration of mast arm traffic signal support structure of various configurations", *Proceedings of the 3rd Amer. Assoc. for Wind Eng. Workshop*, Hyannis, MA.

Johns, K.W. and Dexter, R.J. (1998), "The development of fatigue design load ranges for cantilevered sign and signal support structures", *J. Wind Eng. Ind. Aerod*, **77-78**, 315-326.

Letchford, C.W., Cruzado, H. and Zuo, D. (2008), *Full-scale controlled tests of wind loads on traffic signal structures*, Texas Dept. of Transportation, Austin, TX, Tech. Rep.

National Oceanic and Atmospheric Administration (NOAA) (1998), Department of Defense, Federal Aviation Administration, United States Navy, Automated Surface Observing System (ASOS) User's Guide .

NYSDOT (2010), *Determining remaining fatigue life of in-situ mast-arm traffic signal structures*, Request for Proposals SPR No. C-10-07.

The Integrated Surface Database (ISD), National Climatic Data Center (NCDC), U.S. Department of Commerce http://www.ncdc.noaa.gov/oa/climate/isd/index.php

T. P. Products (2013), "Traffic signal standards "TR" Series".

Wikipedia (2005), "Vort2.gif", http://en.wikipedia.org/wiki/Vortex_shedding.

JH